



velocity  $v$  are taken from reference (5) and as shown in Table1. Substituting these into Eqs. (1) and (2),  $Nu_m$  is given from  $\alpha_m$ . Namely,

$$\alpha = 1.523 \times 10^3 W/m^2 \cdot K \quad (\text{When } u=2\text{mm/s}). \quad (3)$$

$$\alpha = 11.27 \times 10^3 W/m^2 \cdot K \quad (\text{When } u=25\text{mm/s}). \quad (4)$$

Figure2 shows numerical solutions for heat transfer coefficient for  $u = 25\text{mm/s}$ . The maximum value  $\alpha = 18.13 \times 10^3 W/m^2 \cdot K$  appears at  $x = -85\text{mm}$ , while the minimum value  $\alpha = 3.675 \times 10^3 W/m^2 \cdot K$  appears at  $x = 57.8\text{mm}$ . The average value is  $\alpha_m = 10.9 \times 10^3 W/m^2 \cdot K$ , which is in good agreement with Eq. (4).

### 2.3 ANALYSIS MODEL

In this analysis, the total number of nodes is 20816 and the number of elements is 19500. Table2 shows mechanical properties of ceramics. Here, Sialon is considered as material of the tube. Temperature of the molten aluminum is assumed as  $750^\circ\text{C}$ , and the initial temperature of the tube is assumed as  $20^\circ\text{C}$ . Table 3 shows the assumption of heat transfer. Here, 4-node quadrilateral elements will be employed for FEM analysis.

Table 1 the Physical Property of Molten Aluminum at  $750^\circ\text{C}$

Physical Property (dimension)	Al ( $750^\circ\text{C}$ )
Thermal conductivity ( $\lambda$ (W/m K))	112.2
Roll diameter (D(m))	0.17
Kinematics viscosity ( $V$ ( $\text{mm}^2/\text{s}$ ))	0.967
Isobaric specific heat ( $C_p$ (Kj/kg K))	1.1
Viscosity ( $\eta$ (mPa s))	2.2
Constants in Eq. (1) when	
$Re = 1 \times 10^3 - 2 \times 10^5 (C_1)$	0.26
Constants in Eq. (1) when	
$Re = 1 \times 10^3 - 2 \times 10^5 (n)$	0.6

Table 2 Mechanical Property of Ceramics

Physical Property (dimension)	Sialon
Thermal conductivity (W/m K)	17
Specific Heat (J/kg K)	650
Coefficient of Linear Expansion (1/K)	$3.0 \times 10^{-6}$
Young's Modulus (GPa(Kgf/mm <sup>2</sup> ))	294 (29,979)
Specific Weight	3.26
Poisson's Ratio	0.27
Point Bending Strength (MPa (Kgf/mm <sup>2</sup> ))	1050 (10,296)
Fracture Toughness (MN/m <sup>3/2</sup> )	7.5

## 3 Results and Discussion

### 3.1 THE THERMAL STRESS FOR THE VERTICAL TUBE DIPPING SLOWLY AT U=2MM/S

The tube model in the low pressure casting

machine as shown in Figure1.a is considered when the tube is dipped into the crucible slowly,  $u=2\text{mm/s}$ . Here total of 19500 elements with 20816 nodes have been used. When  $u=2\text{mm/s}$ ,  $\alpha_m = 1.523 \times 10^3 W/m^2 \cdot K$  as shown in Eq. (3) are applied for the whole surface,  $r=85\text{mm}$  and  $z=1300\text{mm}$ , since it takes 328s for completely dipping, 16 levels of partially dipping models are considered as shown in the Table 3, and  $\alpha_m = 1.523 \times 10^3 W/m^2 \cdot K$  is applied to the surface touching molten aluminum. Then, the results are shown in Figure3. Figure3 indicates the maximum tensile principle stress  $\sigma_1$ , maximum compressive principle stress  $\sigma_3$  and maximum stresses components  $\sigma_r, \sigma_\theta, \sigma_z$ . Since the maximum shear stresses  $\tau_{rz}, \tau_{\theta z}, \tau_{r\theta}$  are within 25% of  $\sigma_{z\text{max}}$ , only the largest shear stress  $\tau_{rz}$  is

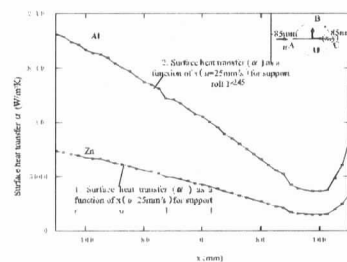


Figure.2 surface heat transfer as function of  $x(u=25\text{mm/s})$

indicated. From Figure3 it is seen that  $\sigma_{z\text{max}}$  coincides with  $\sigma_1$  at  $t=20.5\text{s}$ , and  $\sigma_{z\text{min}}$  coincides with  $\sigma_3$  at  $t=165\text{s}$ . As shown in Figure3, therefore only  $\sigma_{z\text{max}}$  and  $\sigma_{z\text{min}}$  will be discussed because they are almost equivalent to the maximum stresses  $\sigma_1$  and  $\sigma_3$ , respectively. The stress  $\sigma_{z\text{max}}$  has the peak value of 128 MPa at 20.5s.

### 3.2 THE THERMAL STRESS FOR THE VERTICAL TUBE DIPPING FAST AT U=25MM/S

The thermal stress is considered when the tube is dipped into the crucible fast,  $u = 25\text{mm/s}$ . Then, the surface heat transfer is assumed in the following way:

1. When  $t=0-60\text{s}$ ,  $\alpha_m = 18.13 \times 10^3 W/m^2 \cdot K$  as shown in Figure2 is applied to the tube surface,  $r=85\text{mm}$ , and also  $\alpha_m = 3.675 \times 10^3 W/m^2 \cdot K$ , which is the minimum value in Figure2, is assumed at the tube.

2. When  $t > 60\text{s}$ ,  $\alpha = 3.675 \times 10^3 W/m^2 \cdot K$  is assumed for all the surface. Then, the results are shown in Figure4.

As shown in Figure4 the maximum stresses increase in a short time, and has a peak value of 219 MPa at  $t=1.31\text{s}$ . Namely, the larger stress appears shortly compared to the case of  $u = 2\text{mm/s}$ . It may be concluded that vertical dipping is slow in order to reduce the thermal stresses.

### 3.3 THE THERMAL STRESS FOR THE HORIZONTAL TUBE DIPPING SLOWLY U=2MM/S

The horizontal tube dipping into molten aluminum as shown in Figure 1.b is considered when the tube is dipped into the crucible slowly at  $u = 2\text{mm/s}$ . Here, total of 45000 elements with 55986 nodes have been used. When  $u = 2\text{mm/s}$ ,  $\alpha_m = 1.523 \times 10^3 \text{W/m}^2 \cdot \text{K}$  as shown in Eq. (3) are applied for the whole surface,  $r=85\text{mm}$  and  $z=1300\text{mm}$ , since it takes 210s for completely dipping, 6 levels of partially dipping models are considered as shown in the Table 3, and  $\alpha_m = 1.523 \times 10^3 \text{W/m}^2 \cdot \text{K}$  is applied to the surface touching molten aluminum. Figure 5 shows the

Table 3 Assumption of heat transfer  $\alpha (\text{W/m}^2 \cdot \text{K})$

Model	Stalk for Sialon model under Horizontal dipping (Molten Al T=750°C)	Stalk for Sialon model under Vertical dipping (Molten Al T=750°C)
$u=2\text{mm/s}$	<ul style="list-style-type: none"> <li>z=1300 mm</li> <li>r=85 mm</li> <li><math>\alpha = 1.523 \times 10^3 (\text{W/m}^2 \cdot \text{K})</math></li> <li>Level 4</li> <li>Level 2</li> </ul>	<ul style="list-style-type: none"> <li>z=1300 mm</li> <li>r=85 mm</li> <li><math>\alpha = 1.523 \times 10^3 (\text{W/m}^2 \cdot \text{K})</math></li> <li>Level 16</li> <li>Level 8</li> <li>Level 7</li> </ul>
$u=25\text{mm/s}$	<ul style="list-style-type: none"> <li>z=1300 mm</li> <li>r=85 mm</li> <li><math>\alpha = 18.13 \times 10^3 (\text{W/m}^2 \cdot \text{K})</math></li> <li>z=60 mm</li> <li><math>\alpha = 3.675 \times 10^3 (\text{W/m}^2 \cdot \text{K})</math></li> </ul>	<ul style="list-style-type: none"> <li>z=1300 mm</li> <li>r=85 mm</li> <li><math>\alpha = 18.13 \times 10^3 (\text{W/m}^2 \cdot \text{K})</math></li> <li>z=60 mm</li> <li><math>\alpha = 3.675 \times 10^3 (\text{W/m}^2 \cdot \text{K})</math></li> </ul>

results of thermal stress. From Figure 5 it is seen that  $\sigma_{1\text{max}} = 258 \text{MPa}$  at  $t=75\text{s}$ , and  $\sigma_{3\text{max}} = -310 \text{MPa}$  at  $t=75\text{s}$ .

### 3.4 THE THERMAL STRESS FOR THE STALK UNDER HORIZONTAL DIPPING FAST AT $U=25\text{MM/S}$

When the tube is dipped into the crucible fast,  $u = 25\text{mm/s}$ , the results is similar to the case under vertical dipping. Here, the surface heat transfer is assumed in the following way:

1. When  $t=0-60\text{s}$ ,  $\alpha_m = 18.13 \times 10^3 \text{W/m}^2 \cdot \text{K}$  as shown in Figure 2 is applied at the tube surface,  $r=85\text{mm}$ , and also  $\alpha_m = 3.675 \times 10^3 \text{W/m}^2 \cdot \text{K}$ , which is the minimum value in Figure 2, is assumed at the tube.

2. When  $t>60\text{s}$ ,  $\alpha = 3.675 \times 10^3 \text{W/m}^2 \cdot \text{K}$  is assumed for the whole surface. Then, the results are shown in Figure 6.

As shown in Figure 6 the maximum stresses increase in a short time, and has a peak value of  $\sigma_{\theta\text{max}} = 222\text{MPa}$  at  $t=1.5\text{s}$ . Namely, the larger stress appears compared to the case of  $u = 2\text{mm/s}$ . Therefore a tube should dip fast  $u = 25\text{mm/s}$  rather than slowly  $u = 2\text{mm/s}$  to reduce the thermal stress.

### 3.5 COMPARISON BETWEEN THE RESULTS OF STALK UNDER VERTICAL AND HORIZONTAL DIPPING

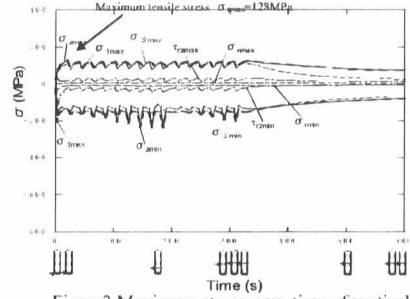


Figure 3 Maximum stresses vs. time of vertical tube ( $u=2\text{mm/s}$ )

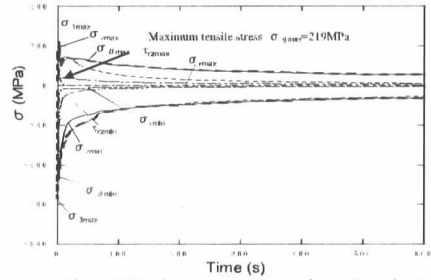


Figure 4 Maximum stresses vs. time of vertical tube ( $u=25\text{mm/s}$ )

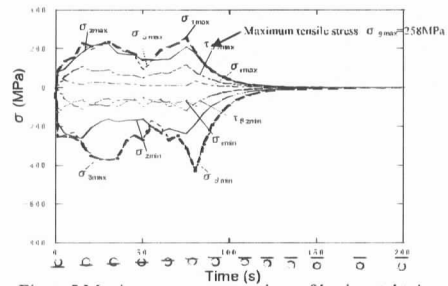


Figure 5 Maximum stresses vs. time of horizontal tube ( $u=2\text{mm/s}$ )

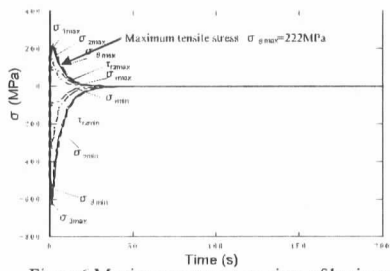


Figure 6 Maximum stresses vs. time of horizontal tube ( $u=25\text{mm/s}$ )

Sialon has been used as the tube because it has high temperature and corrosion resistances. The results of vertical and horizontal tube are indicated in Figures 3-6. The thermal stress of vertical tube for  $u = 2\text{mm/s}$  has a peak value of  $\sigma_{\theta\text{max}} = 128\text{MPa}$  at  $t=20.5\text{s}$ , which is lower than the value of horizontal tube by about 50%. Namely, the thermal stress for the vertical tube is smaller than the one of horizontal tube.

Figure 7.a shows temperature and maximum stress at  $t=20.5\text{s}$  where maximum  $\sigma_{\theta\text{max}} = 128\text{MPa}$  appears when the tube dips slowly. Figure 7.b shows temperature and maximum stress at  $t=1.3\text{s}$  where maximum  $\sigma_{\theta\text{max}} = 219\text{MPa}$  appears when the tube dips

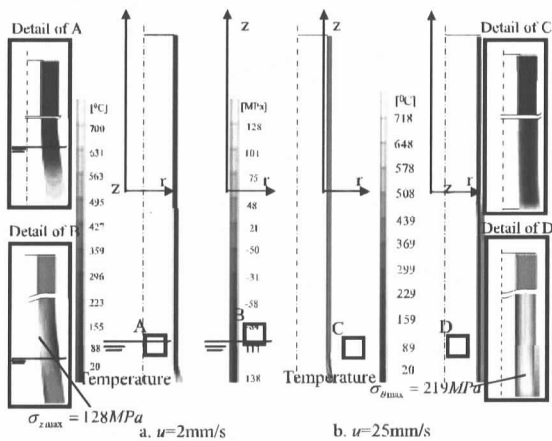


Figure 7 Temperature, stress and displacement at maximum stress occurred for vertical tube ( $u=2\text{mm/s}$  at time  $t=20.5\text{s}$  and  $u=25\text{mm/s}$  at time  $t=1.31\text{s}$ , displacement  $u \times 50$ )

fast. For the slowly dipping ( $u = 2\text{mm/s}$ ), the maximum stress  $\sigma_z$  appears at the inside surface of

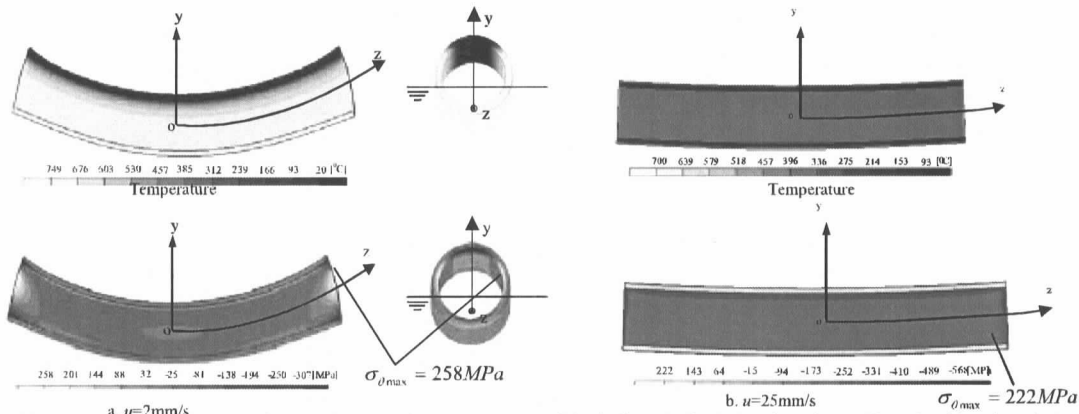


Figure 8 Temperature, stress and displacement at maximum stress occurred for horizontal tube ( $u=2\text{mm/s}$  at time  $t=75\text{s}$  and  $u=25\text{mm/s}$  at time  $t=1.5\text{s}$ , displacement  $u_y \times 50$ )

the tube  $r=70\text{mm}$  just above the surface of molten aluminum. This is due to the bending moment caused by the thermal expansion of the dipping portion of the tube. On the other hand, for the fast dipping ( $u = 25\text{mm/s}$ ),  $\sigma_{z\text{max}}$  appears at the inside of the thickness. This is due to the large temperature difference appearing in the thickness direction.

Figure 8.a shows temperature and maximum stress distributions where  $\sigma_{z\text{max}}=258\text{MPa}$  appears when the stalk dips slowly at 75s. Figure 8.b shows temperature and maximum stress distributions where  $\sigma_{\theta\text{max}}=222\text{MPa}$  appears when the stalk dips fast at  $t=1.5\text{s}$ . For slowly dipping, as shown in Figure 8.a,  $\sigma_{\theta\text{max}}$  appears at the end of the tube  $z = \pm 650\text{mm}$  differently from other cases. In this case,  $\sigma_{\theta\text{max}}$  appears due to asymmetric deformation. For fast dipping as shown in Figure 8.b, the temperature and stress distribution is similar to Figure 7.b. This is because when dipping fast, the deformation is almost axisymmetric.

For vertical tube, fast dipping has a higher

maximum stress than slowly dipping. On the other hand for horizontal dipping, fast dipping has a lower maximum stress than slower dipping. This is because for horizontal tube large asymmetric deformation causes large  $\sigma_{\theta\text{max}}$  at the end of the tube.

#### 4 Conclusions

- (1) For vertical tube, dipping slowly at  $u=2\text{mm/s}$  can reduce the thermal stresses compared with the case of dipping fast at  $u=25\text{mm/s}$ . In other words, when the stalk is set, dipping fast is not suitable for reducing thermal stress.
- (2) However, horizontal tube should be dipped fast in order to reduce the thermal stress.
- (3) When horizontal tube is dipping slowly, large asymmetric deformations cause large  $\sigma_{\theta\text{max}}$  at the end of the tube. If horizontal tube is dipping fast, such large  $\sigma_{\theta\text{max}}$  does not appear because the deformation is almost axisymmetric.

#### References

- (1) Zukauskas A. Heat Transfer form tubes in cross flow. In: Hartnett JP, Irvine Jr TF, editors, Advances in Heat Transfer, vol.8. New York: Academic Press; 1972. p. 131.
- (2) Editorial committee of JSME. Data of heat transfer. Tokyo: JSME; 1986. p.61 [in Japanese].
- (3) Adachi T, Tamura Y, Yoshioka T. Techniques of Automatic Operation in Continuous Galvanizing Line, Kawasaki Steel Technical Report, vol.34; 1996. p. 18-25.
- (4) Nishimura K, Katayama K, Kimura T, Yamaguchi T, Ito M, Newly Develop Techniques for Improving the Quality of Continuous Hot dip Plating Strips, Hitachi Technical Report, vol. 65(2); 1983.p. 121-126 [in Japanese].
- (5) Editorial committee of JSME. Data of heat transfer. Tokyo: JSME; 1986. p.323 [in Japanese].